

RESEARCH ARTICLE

Requirement for scleraxis in the recruitment of mesenchymal progenitors during embryonic tendon elongation

Alice H. Huang^{1,2,*}, Spencer S. Watson¹, Lingyan Wang³, Brendon M. Baker⁴, Haruhiko Akiyama⁵, John V. Brigande³ and Ronen Schweitzer^{1,*}

ABSTRACT

The transcription factor scleraxis (*Scx*) is required for tendon development; however, the function of *Scx* is not fully understood. Although *Scx* is expressed by all tendon progenitors and cells, only long tendons are disrupted in the *Scx*^{-/-} mutant; short tendons appear normal and the ability of muscle to attach to skeleton is not affected. We recently demonstrated that long tendons are formed in two stages: first, by muscle anchoring to skeleton via a short tendon anlage; and second, by rapid elongation of the tendon in parallel with skeletal growth. Through lineage tracing, we extend these observations to all long tendons and show that tendon elongation is fueled by recruitment of new mesenchymal progenitors. Conditional loss of *Scx* in mesenchymal progenitors did not affect the first stage of anchoring; however, new cells were not recruited during elongation and long tendon formation was impaired. Interestingly, for tenocyte recruitment, *Scx* expression was required only in the recruited cells and not in the recruiting tendon. The phenotype of *Scx* mutants can thus be understood as a failure of tendon cell recruitment during tendon elongation.

KEY WORDS: Tendon development, Musculoskeletal, Scleraxis, Mouse

INTRODUCTION

Development of the limb musculoskeletal system requires the coordinated differentiation and growth of the skeleton, muscles and tendons, however, the patterning cues and mechanisms that allow for integrated development are largely unknown. Although it is well established that the primary skeletal structures (i.e. the long bones) and muscles can form independently of one another, a growing body of evidence suggests that the formation of tendons requires signals from the adjacent skeletal and muscle tissues (Arvind and Huang, 2017; Blitz et al., 2009; Chen and Galloway, 2014; Edom-Vovard and Duprez, 2004; Huang, 2017; Kardon, 1998). Tendon function in integrating muscle and skeleton into a unified system suggests that the regulation of tendon growth may be a key mechanism by which the musculoskeletal system maintains coordinated growth to establish proportions optimal for mechanical tension and force transfer. Despite the functional importance of tendons, however, there is still very little known about the cell and molecular events that regulate their growth and development.

In the mouse limb, the distal skeletal segments are controlled by long tendons that extend from muscles in the arm (zeugopod) and insert into skeletal sites within the wrist or paw (autopod) (Watson et al., 2009). Autopod and zeugopod tendons are formed as separate modular units that are independently regulated, such that tendons in one segment can develop in the absence of tendons in the other segment (Huang et al., 2015; Kardon, 1998). While autopod tendon induction depends on cartilage, the zeugopod tendon components are first induced at E12.5 as short-range progenitors that anchor muscle to the skeleton, followed by tendon differentiation and elongation in parallel with skeletal growth. In the absence of muscle, zeugopod tendon induction is initiated, but subsequent differentiation and growth fails at E13.5 and the tendon anlagen are lost (Huang et al., 2015). This biphasic mode of long tendon development (anchoring and elongation) provides a useful framework at the tissue level, but the cellular dynamics and molecular regulators of this process have not been established.

One intriguing marker for tendon is the transcription factor scleraxis (*Scx*), which is expressed by all tendon progenitors and cells, yet its functional role in tendon development remains poorly understood (Murchison et al., 2007; Schweitzer et al., 2001; Yoshimoto et al., 2017). The *Scx*^{-/-} mutant displays a strong tendon phenotype; however, not all tendons are equally affected (Murchison et al., 2007). The long-range tendons of the trunk and limbs are either missing or severely deficient, but short-range anchoring tendons appear normal. Importantly, the ability of tendon to connect muscle to skeleton is not impaired in the absence of *Scx*, as the *Scx*^{-/-} mutant is viable after birth, despite limited mobility due to disruption of the long tendons. This suggests that *Scx* may be functionally important for tendon growth and elongation.

One paradigm underlying tissue and organ development follows a basic assumption that progenitor cells are specified at an early stage and that these cells then differentiate and proliferate to form the final tissue/organ (Gilbert, 2010). There is emerging evidence, however, suggesting that this simple paradigm is not applicable for all tissues/organs. In the joint, it has been shown that joint progenitor cells may be continuously induced and allocated (Shwartz et al., 2016). In this study, we show that tendon elongation in the mouse limb and tail is fueled by recruitment of new mesenchymal progenitors. We further find that *Scx* is not required for tendon anchoring, but *Scx* expression in mesenchymal progenitors is required for their recruitment during tendon elongation, underlying the disruption of long tendons in the *Scx* mutant.

RESULTS

Long tail tendons develop via establishment of a short-range tendon anlage followed by tendon elongation

Integration of the musculoskeletal tissues is first established at E12.5, when short-range anchoring tendons attach muscles to the

¹Research Division, Shriners Hospital for Children, Portland, OR 97239, USA.

²Department of Orthopaedics, Icahn School of Medicine at Mount Sinai, New York, NY 10029, USA. ³Oregon Hearing Research Center, Oregon Health & Science University, Portland, OR 97239, USA. ⁴Department of Biomedical Engineering, University of Michigan, Ann Arbor, MI 48109, USA. ⁵Department of Orthopaedics, Gifu University, Gifu City 501-1194, Japan.

*Authors for correspondence (alice.huang@mssm.edu; schweitz@ohsu.edu)

 A.H.H., 0000-0002-5037-6829

skeleton. Subsequent elongation of the short-range tendon anlage into the zeugopod allows for coordinated development of all musculoskeletal elements during growth (Huang et al., 2015). Although this model was initially conceptualized based on observations in limb tendon development, the limb as a model system poses additional challenges for mechanistic studies due to the complex patterning of several tendons (which are initially formed as fused units that subsequently separate) as well as the modular nature of the autopod and zeugopod segments during tendon development (Huang et al., 2015; Watson et al., 2009). To bypass these complexities, we turned to the tail tendons as a simplified model system to identify the cell and molecular mechanisms underlying anchoring and elongation. Tail tendons are also advantageous because they are the longest tendons in the body and undergo the most dramatic growth during development.

The fully formed mouse tail consists of long tendons that extend from muscles that reside in the base of the tail to each vertebral bone within the tail (Fig. 1A) (Shinohara, 1999). Movement of each skeletal element is governed by dorsal and ventral tendons organized in quadrants (Fig. 1A,B). As all tendons extend from muscles at the base of the tail, the tendons that insert closest to the tip of the tail are much longer than those that insert closer to the base. To determine whether tail tendon development is governed by similar principles of anchoring and elongation, we examined the early stages of tail development. Whole-mount confocal imaging of E13.5 *ScxGFP* embryos showed repeating short-range *ScxGFP*⁺ tendon segments along the tail, attached to their respective vertebral structures (Fig. 1C). The shortest tendon segments were found closest to the tip of the tail (white arrow). Whole-mount immunostaining for myosin heavy chain for muscle showed that each of these short-range tendon segments is directly attached to muscle (Fig. 1C',C''). Between E13.0 and E15.5, there is dramatic

elongation of these short-range tendon segments to form the long-range tendons of the tail, concurrent with skeletal growth (Fig. 1D). These results show that long tail tendons also undergo a developmental process of tendon anchoring followed by tendon elongation, similar to the long tendons of the limb.

Sox9 lineage tracing shows tail tendon elongation is driven by recruitment of new tendon progenitors

Having established that long tail tendons undergo elongation, we next examined the cellular basis for tendon elongation and asked whether the cells driving tendon elongation are completely derived from the early population of anlage progenitors or whether there is subsequent recruitment of new cells. To address this issue, we used *Sox9^{Cre}* to distinguish early tendon progenitors because it has previously been demonstrated that the cells forming the early skeletal insertion site are derived from bipotent *Scx*⁺/*Sox9*⁺ progenitors, established at E12.5 (Blitz et al., 2013; Sugimoto et al., 2013). The transient expression of *Sox9* in early tendon progenitors and the consistent localization of *Sox9* lineage (*Sox9^{lin}*) tendon cells to regions near the skeletal insertion suggested that *Sox9* in tendons may be a distinctive marker for the anchoring anlagen progenitors. We therefore examined the tails of *Sox9^{Cre}* embryos combined with the *Rosa26-TdTomato* (*RosaT*) Cre reporter at E12.5. Imaging by whole-mount confocal microscopy and in transverse sections showed that the *ScxGFP*⁺ tail tendon anlagen are completely derived from *RosaT*⁺, *Sox9^{lin}* cells, demonstrating that *Sox9* is indeed a useful marker for the anchoring tendon in the tail (Fig. 2A,B-B'',C-C'').

As the early tail tendon anlagen is composed of *Sox9^{lin}* progenitors, we used the inducible *Sox9^{CreERT2}* mutant to label these cells at E12.5 via tamoxifen injection and determined whether new tendon progenitors are recruited during tendon elongation. To

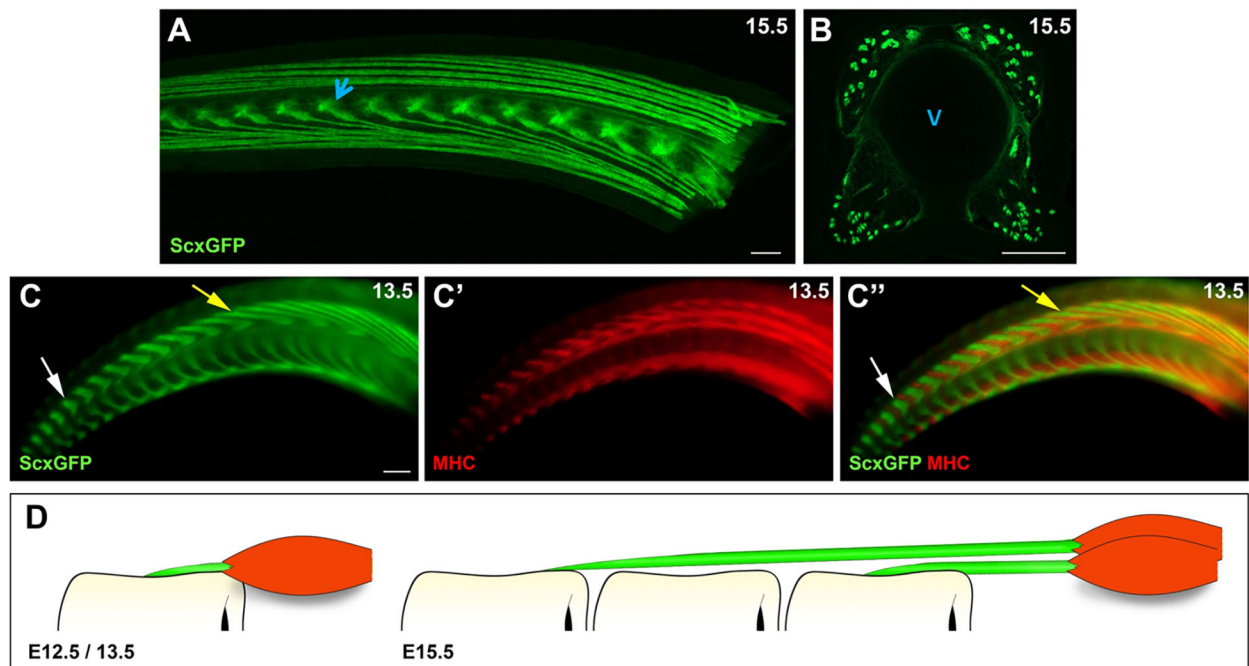


Fig. 1. Long tail tendons develop via anchoring and elongation. (A) Whole-mount confocal and (B) transverse section images of long tail tendons from *ScxGFP* embryos at E15.5. (C) Whole-mount confocal images of short-range tail tendon anlage from *ScxGFP* embryos at E13.5. (C',C'') Whole-mount staining with MHC for muscle and *ScxGFP* and MHC overlays. (D) Schematic of a short tail tendon integrating muscle with skeleton at E12.5/E13.5 and elongated long tail tendons at E15.5. Blue arrow in A indicates an example vertebral body (V in B). Yellow and white arrows highlight proximal and distal tendons, respectively. Scale bars: 200 μ m for whole-mount tails; 100 μ m for E15.5 transverse section in B.

evaluate the distribution of labeled cells along the tendon, we focused our analyses to two distinct regions in the tail in order to (1) follow individual tendons as they insert into the skeleton as well as (2) capture tendons well away from their skeletal insertions. As tail tendons are extremely long and numerous (Fig. 1), we determined that the best region to follow individual tendons as they insert was close to the tail tip (because most of the other tendons would have already inserted proximally). A series of consecutive transverse sections taken across the length of the tail tip at E16.5 showed that tendon cells further from the insertion (tendon 5, L1) are devoid of *Sox9^{lin}* cells, while tendon cells near/at the insertion (tendon 1, L1 and L2; tendon 2, L3 and L4) are strongly composed of *Sox9^{lin}* cells (Fig. 2D,E). To confirm that tendon cells away from the skeletal insertions are non-*Sox9^{lin}*, we also collected sections closer to the tail base where the tendons attach to muscle. Analysis of these sections revealed that the bulk of the tendon midsubstance length was almost completely derived from non-*Sox9^{lin}* cells (*ScxGFP⁺*, *RosaT⁻*), indicating that tendon elongation is likely fueled by recruitment of new progenitors and not by expansion of the original anchoring population (Fig. 2F,G).

As previous studies showed dramatic variability in the contribution of *Sox9^{lin}* cells in tendons (Soeda et al., 2010), we

also examined *Sox9^{Cre}*-labeled tail tendons at E16.5 in transverse sections. To our surprise, *Sox9^{Cre}* lineage tracing showed that the full length of dorsal tail tendons (from skeletal insertion to muscle origin) is almost entirely composed of *Sox9^{lin}* cells (Fig. S1). Notably, ventral tail tendons were composed of largely non-*Sox9^{lin}* cells, which suggested that *Sox9* itself is likely not playing a functional role in tendon development (Fig. S1). This is also supported by other studies showing that deletion of *Sox9* by *Scx^{Cre}* does not result in loss of tendon (Blitz et al., 2013). Collectively, the analyses of *Sox9^{CreERT2}* and *Sox9^{Cre}* tail tendons indicate that the anchoring tendon is initially composed of *Sox9^{lin}* cells, while new tendon progenitors are subsequently recruited during tendon elongation. In addition, these progenitors may be either *Sox9^{lin}* or non-*Sox9^{lin}*.

Conditional deletion of *Scx* shows that *Scx* is required in mesenchymal cells to enable their recruitment during tail tendon elongation

As both the anchoring tendon progenitors and the recruited mesenchymal cells in dorsal tendons are derived from *Sox9^{lin}* progenitors, we next tested *Scx* function using *Sox9^{Cre}* to target both cell populations in dorsal tendons. In *Scx^{-/-}* mutants, tail tendons

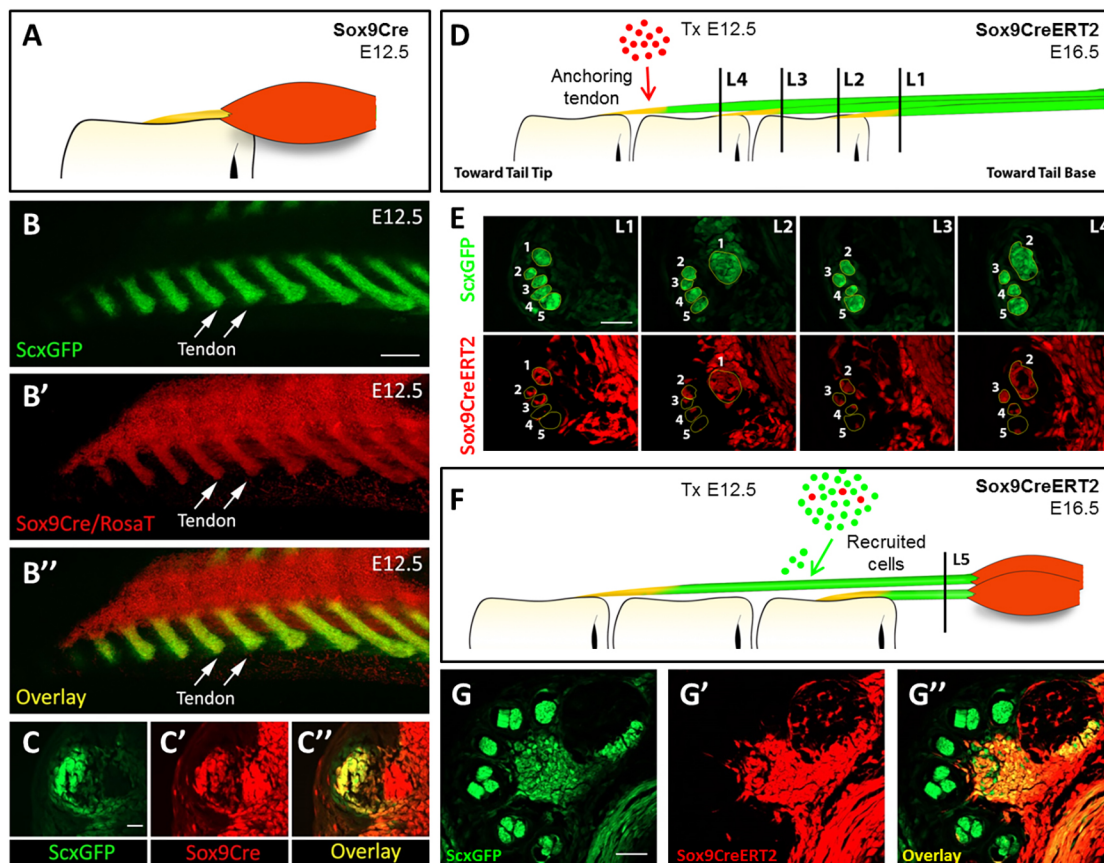


Fig. 2. Tail tendon elongation is enabled by recruitment of new cells. (A) Schematic of *Sox9^{lin}* cell composition of short-range tail tendons labeled by *Sox9^{Cre}* at E12.5 (yellow color indicates both *ScxGFP⁺* and *RosaT⁺*). (B–C'') Whole-mount confocal (B–B'') and transverse section (C–C'') images of *Sox9^{Cre}*; *RosaT*; *ScxGFP* tail tendon anlage at E12.5. (B', C') *RosaT* signal; (B'', C'') *ScxGFP* and *RosaT* overlays. (D) Schematic of *Sox9^{lin}* composition of long tail tendons from *Sox9^{CreERT2}* embryos at E16.5 (tamoxifen at E12.5) highlight *RosaT* labeling of skeletal-tendon insertions. (E) Transverse sections through the distal tail tip of *Sox9^{CreERT2}*; *RosaT*; *ScxGFP* embryos at E16.5; tamoxifen was given at E12.5. Sections collected through level planes shown in D (L1–L4); 1–5 labels follow specific dorsal tendons through the sections. (F) Schematic of *Sox9^{lin}* composition of long tail tendons from *Sox9^{CreERT2}* embryos at E16.5 (tamoxifen at E12.5) highlight the absence of *RosaT* in the tendon body. (G–G'') Transverse sections through tail base of *Sox9^{CreERT2}*; *RosaT*; *ScxGFP* embryos at E16.5; tamoxifen was given at E12.5. Section collected through level plane L5 shown in F. (G', G'') *RosaT*, and *ScxGFP/RosaT* overlays. Scale bars: 200 μ m for E12.5 whole-mount tail (B–B''); 25 μ m for all transverse sections.

are severely disrupted. If *Scx* is required in anchoring progenitors, we expected *Scx^{Sox9Cre}* mutants to phenocopy *Scx^{-/-}* mutants in that new cells will not be recruited, resulting in a failure of tendon elongation. Conversely, if *Scx* is required only in the recruited mesenchymal cells, then mutant cells will be excluded from the elongating tendon. When we examined transverse sections of tails from *Scx^{Sox9Cre}; RosaT* embryos at E18.5, we found that dorsal tail tendons were still present; however, the mutant tendons were much smaller than wild-type tendons (Fig. 3A-D). Analysis of *RosaT* expression showed that mutant dorsal tendons at the midsubstance were almost completely composed of non-*Sox9^{lin}* cells (Fig. 3C,D). Remarkably, these data showed that out of a large population of mutant cells (*RosaT⁺*), only wild-type cells were capable of recruitment, suggesting that *Scx* is required in mesenchymal cells for their recruitment into tendon. Reduced dorsal tendon size in the mutant was likely a result of the restricted availability of wild-type cells in the surrounding milieu, because in wild-type embryos these tendons are fully composed of *Sox9^{lin}* cells. Moreover, as the anchoring tendon is targeted by *Sox9^{Cre}*, this result also indicates that *Scx* function is required exclusively in the recruited mesenchymal cells and not in the recruiting tendon, because loss of *Scx* in the anchoring tendons in the dorsal tail tendons of these mutants did not preclude cell recruitment. Interestingly, the size of ventral tendons (which normally recruit a mix of *Sox9^{lin}* and non-*Sox9^{lin}* cells) appeared relatively normal in *Scx^{Sox9Cre}* mutants, which may be due to the larger availability of wild-type cells in the vicinity of these tendons (Fig. S1).

Conditional deletion and embryonic cell injections show that *Scx* is required for tendon cell recruitment in the limb

Our experiments in the mouse tail showed that tendon elongation is fueled by recruitment of new cells and that *Scx* is required for their recruitment. To determine whether this is a general mechanism for long tendon growth, we evaluated the complex tendons within the limb by whole-mount confocal imaging. Initial analyses of *Sox9^{Cre}; RosaT*; *ScxGFP* limbs showed broad Cre activity in a variety of tissues, including skin and nerves; as a result, *RosaT* expression was

overwhelming in maximum intensity projections and did not reflect true *Sox9^{lin}* cell contribution to tendon (Fig. S2). We therefore developed a non-biased approach using a customized algorithm in Matlab software to eliminate the *RosaT* signal in *ScxGFP*-negative cells, thereby restricting *RosaT* signal to tendon and related connective tissues (Fig. 4A,B). Analysis of *Sox9^{lin}* cells in limb tendons of *Sox9^{Cre}; RosaT* embryos at E12.5 revealed that the short-range tendon anlage that mediate connections between skeleton and muscle are mostly composed of *Sox9^{lin}* cells, similar to our findings for the E12.5 tail. Interestingly, the short-range tendons that integrate the muscles in the zeugopod with their respective autopod tendons are also mostly composed of *Sox9^{lin}* cells (Fig. 4A, Fig. S3). The *Sox9^{lin}* population in tendons was largely restricted to the wrist where the muscles attached, and the autopod components of these tendons were composed of mixed or non-*Sox9^{lin}* cells. When we evaluated *Sox9^{Cre}; RosaT* embryos at a later stage (E16.5), we found a mixed composition of *Sox9^{lin}* and non-*Sox9^{lin}* cells in most tendons within the zeugopod, although the tendon regions near the wrist and elbow remained strongly *RosaT⁺* for most tendons (Fig. 4B,C). Tamoxifen labeling of *Sox9^{lin}* cells at E12.5 showed that most of the tendon at E16.5 was derived from recruited cells, similar to the distribution in the tail tendons (Fig. 4D). Deletion of *Scx* in *Sox9^{lin}* cells using *Sox9^{Cre}* resulted in a dramatic exclusion of mutant cells from the zeugopod tendons, similar to the phenotype observed in the tail (Fig. 5). Limb tendon diameters were noticeably smaller, although not to the same extent as the mutant dorsal tail tendons.

Because of the mixed composition of *Sox9^{lin}* and non-*Sox9^{lin}* cells in limb tendons, we tested the role of cell recruitment and *Scx* function via an additional experimental approach of injecting labeled mesenchymal cells into developing limbs *in utero* and testing the recruitment of such cells into developing tendons. To label limb mesenchyme, we used the *Prx1^{Cre}* driver that targets all cells in the early limb bud mesenchyme. We isolated *RosaT⁺* mesenchymal cells from *Prx1^{Cre}; RosaT*; *ScxGFP* limb buds at E12.5, and directly injected these cells into the limb buds of stage-matched *ScxGFP* embryos via transuterine microinjection (Fig. 6A).

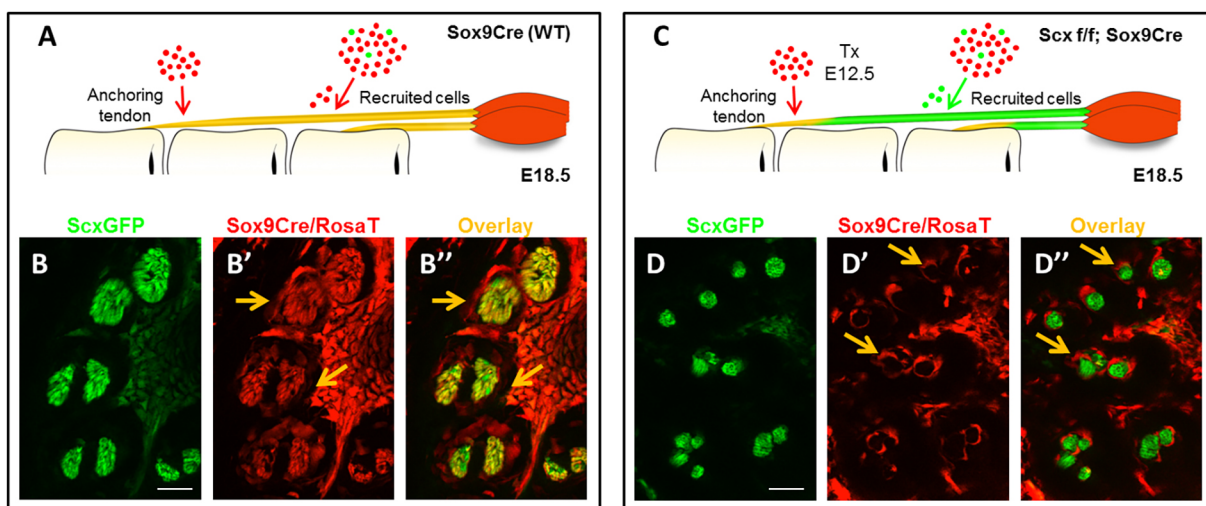


Fig. 3. *Scx* is required for mesenchymal cell recruitment during tail tendon elongation. (A) Schematic of *Sox9^{lin}* cell composition of dorsal tail tendons labeled by *Sox9^{Cre}; RosaT* at E18.5. (B-B'') Transverse section images of *Sox9^{Cre}; RosaT; ScxGFP* long dorsal tail tendons at E18.5. (B', B'') *RosaT* and *ScxGFP/RosaT* overlays. (C) Schematic of *Sox9^{lin}* cell composition of dorsal tail tendons of mutant *Scx^{Sox9Cre}; RosaT; ScxGFP* embryos at E18.5. (D-D'') Transverse section images of *Scx^{Sox9Cre}; RosaT; ScxGFP* dorsal tail tendons at E18.5. (D', D'') *RosaT* and *ScxGFP/RosaT* overlays. Red cells indicate *Sox9^{lin}* tendon cells; green cells indicate non-*Sox9^{lin}* tendon cells. Transverse sections show tendon midsubstance regions. Orange arrows highlight *RosaT⁺/ScxGFP⁻* cells. Scale bars: 25 μ m.

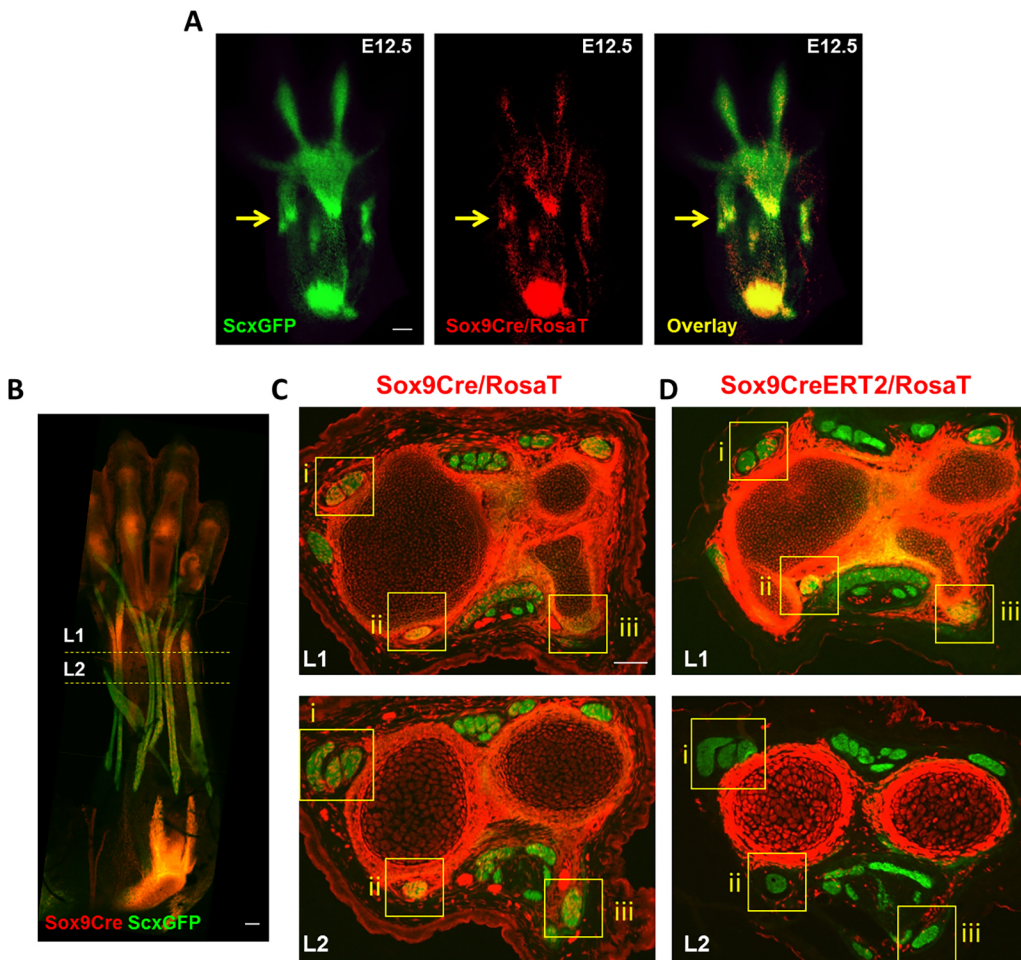


Fig. 4. Limb tendon elongation is also fueled by recruitment of new progenitors. (A) Whole-mount confocal image of *Sox9^{Cre}; Rosa^T; ScxGFP* forelimb at E12.5. (B) Whole-mount confocal image of *Sox9^{Cre}; Rosa^T; ScxGFP* forelimb at E15.5. (C) Transverse section images of wild-type E16.5 *Sox9^{Cre}* labeled tendons at the wrist (L1) and midsubstance (L2) levels shown in B. (D) Transverse section images of wild-type *Sox9^{CreERT2}; Rosa^T; ScxGFP* zeugopod tendons at E16.5 (tamoxifen at E12.5) highlight *Rosa^T* labeling of skeletal-tendon insertions. Comparison of *Sox9^{Cre}* and *Sox9^{CreERT2}* images show that *Sox9^{ln}* cells in the tendon midsubstance are not derived from the short-range tendon but are derived from newly recruited cells. Scale bars: 200 μ m (whole-mount images); 100 μ m (transverse sections).

As only donor cells are labeled, the presence of *Rosa^T* cells incorporated within a tendon would indicate cell recruitment. However, location alone was not sufficient for a *Rosa^T* cell to be considered recruited, unless the labeled cell also adopted a tenogenic fate by expressing *ScxGFP*. Systematic analysis of consecutive

transverse sections taken from digit to elbow showed numerous examples of non-recruited donor cells embedded within the mesenchyme that were not associated with any tendon and did not express *ScxGFP* (white arrows, Fig. 6B,B',C,C'). Occasionally, however, donor cells expressing *ScxGFP* were found within tendon, matching our criteria for recruitment (yellow arrows, Fig. 6B,B'). Out of 26 wild-type injected embryos, seven embryos had at least one positive recruitment event. Positive recruitment involved only one or two cells, and was not limited to any particular tendon or region within a tendon.

Having demonstrated cell recruitment into tendons using transuterine cell injection, we next wanted to test the role of *Scx* in this experimental paradigm. Injecting *Scx^{-/-}* mutant cells into wild-type limbs would closely parallel the genetic experiments described above. However, as we found that injection of wild-type cells into wild-type limbs resulted in modest recruitment efficiency (WT-WT, ~27%), a very large number of injections would be required to determine a definitive failure of the recruitment of *Scx^{-/-}* cells. We therefore opted to perform the complementary experiment by injecting labeled wild-type cells into *Scx^{-/-}* mutant limbs (WT-Mutant) (Fig. 6D). When wild-type cells were injected into mutant limbs, we found that all limbs (4/4) showed positive recruitment events. Moreover, although positive recruitment in the WT-WT experiments produced typically 1-2 cells within a tendon, positive recruitment events in WT-Mutant consisted of massive incorporation of wild-type cells (Fig. 6E',E'',F',F',G',G'). Whole-mount imaging showed extensive *Rosa^T* signal within tendon, which was confirmed via transverse sections showing large

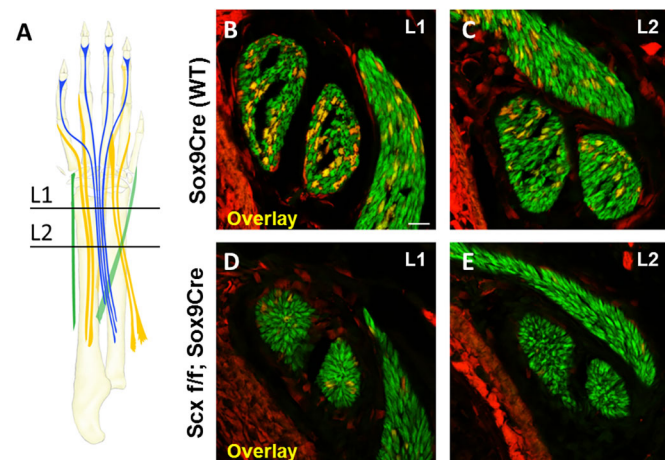


Fig. 5. *Scx* is required for mesenchymal cell recruitment during limb tendon elongation. (A) Schematic image of extensor tendons. (B,C) Transverse section images of wild-type *Sox9^{Cre}*-labeled tendons at the section levels L1 and L2 shown in A. (D,E) Transverse section images of mutant *Scx^{Sox9Cre}* tendons at the section levels L1 and L2 shown in A. Scale bar: 20 μ m.

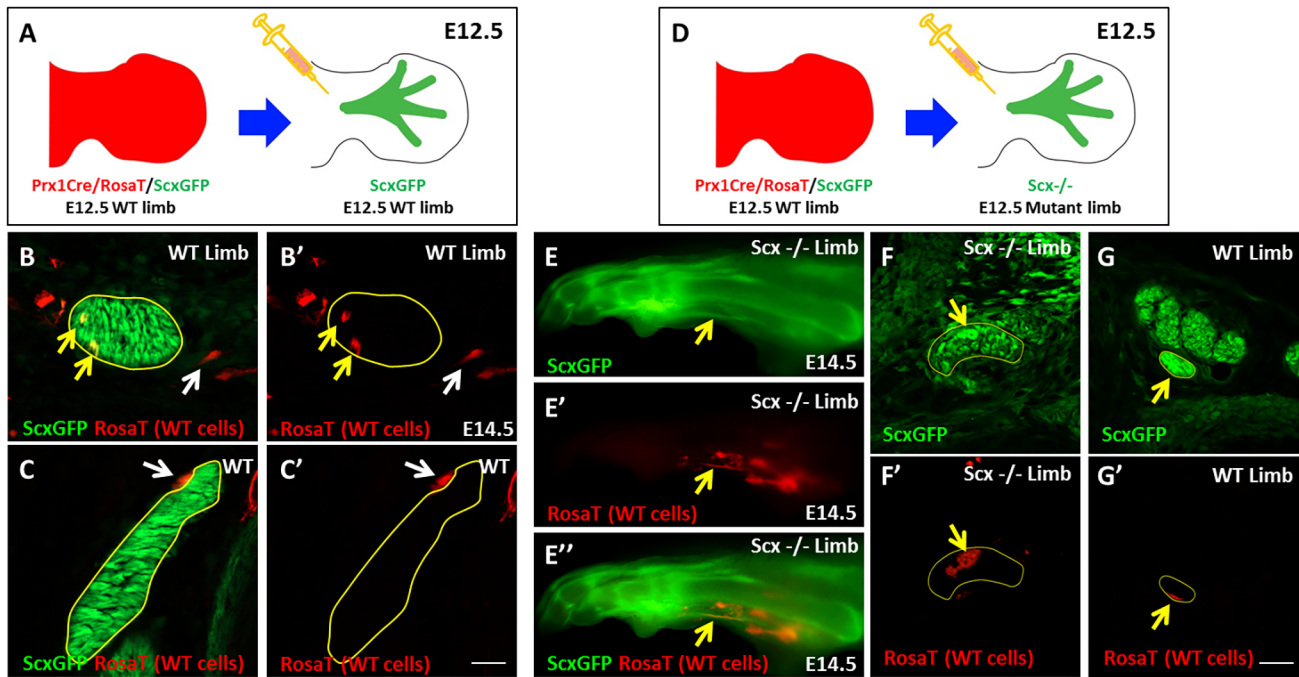


Fig. 6. Transuterine microinjection of limb mesenchymal cells into stage-matched E12.5 limb buds confirms that positive cell recruitment depends on *Scx* function. (A) Schematic of *RosaT*-labeled wild-type donor cell isolation and microinjection into wild-type host limbs. (B) Transverse section through a representative tendon showing positive recruitment of donor cells (yellow arrows, *RosaT*+/*ScxGFP*+) into host tendon. (B') *RosaT* only. White arrows indicate *RosaT*+/*ScxGFP*-negative expression. (C) Transverse section through a representative tendon as an example of non-recruitment, indicated by *RosaT*+/*ScxGFP*-negative expression (white arrow). (C') *RosaT* only. (D) Schematic of *RosaT*-labeled wild-type donor cell isolation and microinjection into mutant *Scx*^{-/-} host limbs. (E-E'') Whole-mount *Scx*^{-/-} limb shows extensive recruitment of wild-type *RosaT* donor cells into tendon (yellow arrows). (F-F'') Transverse sections through mutant (F,F') and wild-type (G,G') tendons show massive and minimal recruitment of wild-type *RosaT*+/*ScxGFP*+ donor cells, respectively (yellow arrows). Data are representative of 26 wild-type embryos and four *Scx*^{-/-} mutant embryos. Scale bars: 25 μ m.

numbers of recruited cells for several consecutive sections, highlighting preferential recruitment of injected wild-type cells in an environment where most mesenchymal cells are *Scx*^{-/-} and therefore cannot be recruited to the tendon. Collectively, these results indicate that cell recruitment is a driving force in tendon elongation and that *Scx* function is required in the mesenchymal cells that are recruited. The ability of *Scx*^{-/-} tendons to recruit wild-type cells further shows that for cell recruitment, *Scx* activity is required exclusively in the recruited cells and there is no role for *Scx* activity in the recruiting tendon.

DISCUSSION

In this study, we show that the long tendons in the body are typically formed by anchoring and elongation, and further identify a fundamental mechanism underlying elongation. We show that additional mesenchymal cells are recruited after induction of the anchoring tendon, which fuels the dramatic extension of long tendons during growth. In addition, *Scx* expression in mesenchymal cells is required for their recruitment, thus establishing a new and crucial function for this essential tendon transcription factor (Fig. 7).

Scx was the first transcription factor identified for tendons, and to date remains the earliest known marker for distinguishing tendon and connective tissue progenitors during embryonic development (Chen and Galloway, 2014; Schweitzer et al., 2001). The early and distinctive expression of *Scx* initially suggested that *Scx* may be a master regulator of the tendon cell fate; however, analyses of the *Scx*^{-/-} mutant subsequently revealed that tendons can still develop in the absence of *Scx*, although many of the tendons are grossly impaired (Murchison et al., 2007; Schweitzer et al., 2001). One confounding aspect of the *Scx*^{-/-} mutant was the divergent phenotypes of two types of tendons, which can be generally classified as short-range and long-range tendons. Although short-range tendons (such as the intrinsic lumbrical tendons of the autopod or the flattened tendon sheets connecting the intercostal muscles to the ribs) are completely unaffected in the *Scx*^{-/-} mutant, long-range tendons (such as the long tendons of the limbs and tail) are severely reduced or missing. In the context of long tendon formation, we now demonstrate that the *Scx*^{-/-} phenotype is a failure of tendon elongation, and, more specifically, a failure of tendon cell recruitment during elongation. This is consistent with

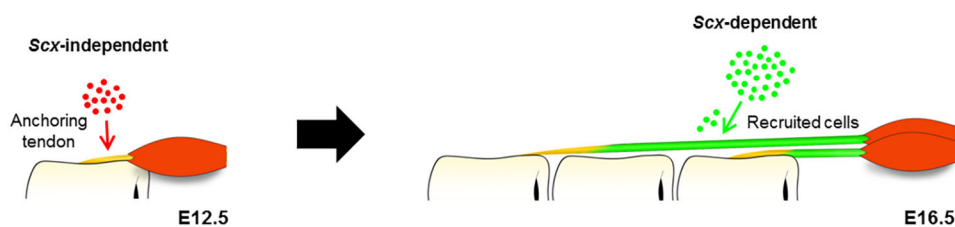


Fig. 7. Model of cell recruitment and *Scx* dependency during long tendon elongation. Schematic of *Scx*-independent anchoring and *Scx*-dependent elongation phases of long tendon development. Red cells indicate *Sox9*^{intj}/*ScxGFP* tendon cells that make up the early anchoring tendon. Subsequently, tendon cells (green) are recruited to enable long tendon growth.

our previous results, which showed normal tendon induction at E12.5 in the *Scx*^{-/-} mutant (during the stage of tendon anchoring), with the manifestation of the tendon phenotype at E13.5 (during the stage of tendon cell recruitment and elongation) (Murchison et al., 2007). In the current study, we also found that deletion of *Scx* in the early population of *Sox9*^{lim} anchoring tendon progenitors at E12.5 did not negate the ability of these cells to subsequently recruit wild-type cells, further supporting the specific activity of *Scx* in the newly recruited mesenchymal cells.

Although we have identified this new and exciting function for *Scx*, it also plays other roles in tendon biology. For example, it has been shown that *Scx* drives expression of *Colla1*, and collagen matrix content is greatly reduced in *Scx*^{-/-} tendons, indicating that *Scx* may also have a later role in tendon matrix synthesis (Léjard et al., 2007; Murchison et al., 2007). The loss of the flexor digitorum profundus tendons in the metacarpal regions of the autopod also suggests a failure of progenitor cell condensation, independent of tendon elongation. Finally, it has previously been shown that *Scx* drives *Bmp4* expression in bone eminence progenitor cells, which is required for cartilage differentiation to form the secondary skeletal structures, such as bone ridges and tuberosities (Blitz et al., 2013, 2009).

Although in this study we used the expression of *Sox9* as a fortuitous marker of early tendon progenitor cells, we found no evidence for a functional role for *Sox9* in either tendon cell anchoring or recruitment during elongation. This is consistent with previous reports, which showed that long tendons are not noticeably disrupted in *Sox9*^{ScxCre} mutants, although the skeletal entheses and tuberosities were lost. In both our tail and limb models, *Sox9*^{lim} and non-*Sox9*^{lim} cells can be recruited into tendons. However, although the composition of *Sox9*^{lim} cells varied dramatically between tendons, the relative composition of *Sox9*^{lim} cells was remarkably constant for each tendon. For example, the dorsal tendons of the tail are always highly composed of *Sox9*^{lim} cells, whereas the ventral tendons are of mixed composition, suggesting that cell recruitment is likely driven by proximity of mesenchymal cells to the growing tendon. In cases where most surrounding cells are from *Sox9*^{lim}, the tendon would be heavily composed of such cells. Consistent with this hypothesis, in the *Scx*^{Sox9Cre} mouse, where *Scx* mutant cells are no longer recruited, tendon size is reduced only in tendons that normally incorporate a large number of *Sox9*^{lim} cells. Consequently, the tendon phenotype of *Scx*^{Sox9Cre} is significantly milder than that of *Scx*^{-/-} tendons in which several long tendons are lost (including all of the long tendons of the tail), likely due to the ability of *Scx*^{Sox9Cre} tendons to still recruit wild-type cells and maintain structural integrity.

The long tendons of the limb and body are a common anatomic feature in mammalian species, but are not universal across tetrapod clads. In more primitive vertebrates such as amphibians, the zeugopod and tail are highly muscular and short tendons mediate the attachment of these muscles to the skeleton (Diogo et al., 2009) (Ashley-Ross, 1992; Diogo et al., 2009; Walthall and Ashley-Ross, 2006). While long tendons are observed in the amphibian autopod, the developmental program governing the autopod tendons is distinct from that of the long zeugopod tendons, and elongation of autopod tendons may involve divergent mechanisms (Huang et al., 2015). While cell recruitment appears to be a fundamental mechanism driving elongation, it is not clear whether recruitment is part of the original mechanism underlying all tendon formation or whether it is a later evolutionary addition specific to the new developmental program regulating long tendon elongation. From a functional perspective, the shift from short to long tendons may be

advantageous. It has been shown that increasing the length of tendons relative to the length of muscle fascicles increases the energy storage capacity of tendons, enhancing muscle function while reducing the metabolic cost of muscle contraction (Alexander, 2002). Interestingly, cell recruitment does not occur as a substitute for tenocyte proliferation (which is sustained throughout the stages of tendon elongation), but is an additional mechanism for generating new cells. This indicates that proliferation alone may be insufficient for the tendon to keep pace with the growth of the underlying skeletal structures. The dramatic extension of the tendons during evolution may have necessitated a new, additional cellular mechanism for growth, to enable the remarkable increase (and variation) in limb length that occurred through mammalian evolution.

MATERIALS AND METHODS

Mice

Existing mouse lines used in these studies have been previously described: *ScxGFP* tendon reporter (Pryce et al., 2007), *Sox9*^{Cre} (Akiyama et al., 2005), *Sox9*^{CreERT2} (Soeda et al., 2010), *Scx*^{-/-} (Murchison et al., 2007), *Scx*^{fl/fl} (Murchison et al., 2007), *Prx1*^{Cre} (Logan et al., 2002) and *Ai14 Rosa26-TdTomato* reporter (*RosaT*) (Madisen et al., 2010). All mice were crossed with *ScxGFP* to enable visualization of tendon cells.

Limb bud cell isolation and transuterine microinjection into E12.5 limbs

Stage-matched timed matings were set for donor embryos (*Prx1*^{Cre}; *RosaT*; *ScxGFP*) and host embryos (*ScxGFP* or *Scx*^{-/-}; *ScxGFP*). On the day of injection, *RosaT*⁺; *ScxGFP*⁺ forelimb and hindlimb buds were isolated from E12.5 donor embryos and rinsed in sterile PBS. Limb bud cells were isolated by incubation in digestion solution (0.1% collagenase, 0.1% trypsin in PBS) at 37°C for 10 min. Cells were then resuspended in DMEM at a concentration of 1.5×10⁶ cells/ml and kept on ice until injection. For injections, the uterine horns of pregnant dams were externalized by ventral laparotomy and transilluminated to visualize the host E12.5 embryo (Gubbels et al., 2008; Huang et al., 2013; Wang et al., 2012). Cell solution (10 nl) was microinjected through the uterus into the presumptive wrist region of the nascent limb. Host embryos with injected limbs were harvested at E14.5 and whole-mount limbs were visually scanned for the presence of *RosaT*⁺ signal, which is indicative of successful injection. Limbs showing any positive expression were then processed for histology and cryosectioned from digit tips to elbow. Every section was collected and inspected to identify recruited cells into tendon.

Histology

Standard protocols for whole-mount and section immunostaining were performed as previously described (Murchison et al., 2007). Patterning of limb and tail tendons, and muscles was acquired in serial transverse sections (Watson et al., 2009). A monoclonal antibody for My32 (Sigma-Aldrich M4276, 1:750) was used to detect muscle-specific type II myosin heavy chain (MHC).

Whole-mount confocal microscopy and image processing

Mouse forelimbs or tails from E12.5 to E15.5 were fixed in 4% paraformaldehyde overnight at 4°C. Following fixation, whole-mount immunostaining for MHC was carried out for E12.5 and E13.5 limbs and tails as previously described (DeLaurier et al., 2006). Tissues were then incubated in Sca/e2 solution at 4°C until cleared (Hama et al., 2011). A Zeiss LSM780 laser scanning confocal microscope was used to acquire 10 tiled z-stack images. Image processing was carried out using Zeiss Zen software to stitch tiles and obtain maximum intensity projection images. Transverse sections were imaged using the Zeiss AxioImager with Apotome for optical sectioning. As *Sox9*^{Cre} labeling is broad in the limb, whole-mount confocal *Sox9*^{Cre}; *RosaT*; *ScxGFP* images were processed using custom MATLAB software to eliminate non-*ScxGFP* contributions to better enable visualization of *Sox9*^{lim} cells in tendon.

Acknowledgements

We thank Brian Pryce for helpful discussions and technical assistance.

Competing interests

The authors declare no competing or financial interests.

Author contributions

Conceptualization: A.H.H., R.S.; Methodology: A.H.H., L.W., J.V.B., R.S.; Software: B.M.B.; Validation: A.H.H., B.M.B., J.V.B., R.S.; Formal analysis: A.H.H., J.V.B.; Investigation: A.H.H., S.S.W., L.W., J.V.B., R.S.; Resources: H.A., J.V.B., R.S.; Data curation: A.H.H.; Writing - original draft: A.H.H., R.S.; Writing - review & editing: A.H.H., R.S.; Visualization: A.H.H., R.S.; Supervision: R.S.; Project administration: R.S.; Funding acquisition: A.H.H., R.S.

Funding

This work was supported by the National Institutes of Health/National Institute of Arthritis and Musculoskeletal and Skin Diseases (R01AR055640 and R01AR055973 to R.S.; R01DC008595 to J.V.B.), by Shriners Hospitals for Children (85410-POR-14 to R.S.) and by the Arthritis Foundation (to A.H.H.). Deposited in PMC for release after 12 months.

Supplementary information

Supplementary information available online at <http://dev.biologists.org/lookup/doi/10.1242/dev.182782.supplemental>

References

- Akiyama, H., Kim, J.-E., Nakashima, K., Balmes, G., Iwai, N., Deng, J. M., Zhang, Z., Martin, J. F., Behringer, R. R., Nakamura, T. et al. (2005). Osteochondroprogenitor cells are derived from Sox9 expressing precursors. *Proc. Natl. Acad. Sci. USA* **102**, 14665-14670. doi:10.1073/pnas.050475102
- Alexander, R. M. (2002). Tendon elasticity and muscle function. *Comp. Biochem. Physiol. A Mol. Integr. Physiol.* **133**, 1001-1011. doi:10.1016/S1095-6433(02)00143-5
- Arvind, V. and Huang, A. H. (2017). Mechanobiology of limb musculoskeletal development. *Ann. N. Y. Acad. Sci.* **1409**, 18-32. doi:10.1111/nyas.13427
- Ashley-Ross, M. A. (1992). The comparative myology of the thigh and crus in the salamanders *Ambystoma tigrinum* and *Dicamptodon tenebrosus*. *J. Morphol.* **211**, 147-163. doi:10.1002/jmor.1052110204
- Blitz, E., Viukov, S., Sharir, A., Schwartz, Y., Galloway, J. L., Pryce, B. A., Johnson, R. L., Tabin, C. J., Schweitzer, R. and Zelzer, E. (2009). Bone ridge patterning during musculoskeletal assembly is mediated through SCX regulation of Bmp4 at the tendon-skeleton junction. *Dev. Cell* **17**, 861-873. doi:10.1016/j.devcel.2009.10.010
- Blitz, E., Sharir, A., Akiyama, H. and Zelzer, E. (2013). Tendon-bone attachment unit is formed modularly by a distinct pool of Scx- and Sox9-positive progenitors. *Development* **140**, 2680-2690. doi:10.1242/dev.093906
- Chen, J. W. and Galloway, J. L. (2014). The development of zebrafish tendon and ligament progenitors. *Development* **141**, 2035-2045. doi:10.1242/dev.104067
- DeLaurier, A., Schweitzer, R. and Logan, M. (2006). Pitx1 determines the morphology of muscle, tendon, and bones of the hindlimb. *Dev. Biol.* **299**, 22-34. doi:10.1016/j.ydbio.2006.06.055
- Diogo, R., Abdala, V., Aziz, M. A., Lonergan, N. and Wood, B. A. (2009). From fish to modern humans - comparative anatomy, homologies and evolution of the pectoral and forelimb musculature. *J. Anat.* **214**, 694-716. doi:10.1111/j.1469-7580.2009.01067.x
- Edom-Vovard, F. and Duprez, D. (2004). Signals regulating tendon formation during chick embryonic development. *Dev. Dyn.* **229**, 449-457. doi:10.1002/dvdy.10481
- Gilbert, S. F. (2010). *Developmental Biology*, 9th edn. Sunderland, MA: Sinauer Associates.
- Gubbels, S. P., Woessner, D. W., Mitchell, J. C., Ricci, A. J. and Brigande, J. V. (2008). Functional auditory hair cells produced in the mammalian cochlea by in utero gene transfer. *Nature* **455**, 537-541. doi:10.1038/nature07265
- Hama, H., Kurokawa, H., Kawano, H., Ando, R., Shimogori, T., Noda, H., Fukami, K., Sakaue-Sawano, A. and Miyawaki, A. (2011). Scale: a chemical approach for fluorescence imaging and reconstruction of transparent mouse brain. *Nat. Neurosci.* **14**, 1481-1488. doi:10.1038/nn.2928
- Huang, A. H. (2017). Coordinated development of the limb musculoskeletal system: Tendon and muscle patterning and integration with the skeleton. *Dev. Biol.* **429**, 420-428. doi:10.1016/j.ydbio.2017.03.028
- Huang, A. H., Riordan, T. J., Wang, L., Eyal, S., Zelzer, E., Brigande, J. V. and Schweitzer, R. (2013). Repositioning forelimb superficialis muscles: tendon attachment and muscle activity enable active relocation of functional myofibers. *Dev. Cell* **26**, 544-551. doi:10.1016/j.devcel.2013.08.007
- Huang, A. H., Riordan, T. J., Pryce, B., Weibel, J. L., Watson, S. S., Long, F., Lefebvre, V., Harfe, B. D., Stadler, H. S., Akiyama, H. et al. (2015). Musculoskeletal integration at the wrist underlies the modular development of limb tendons. *Development* **142**, 2431-2441. doi:10.1242/dev.122374
- Kardon, G. (1998). Muscle and tendon morphogenesis in the avian hind limb. *Development* **125**, 4019-4032.
- Léjard, V., Brideau, G., Blais, F., Salincarnboriboon, R., Wagner, G., Roehrl, M. H. A., Noda, M., Duprez, D., Houillier, P. and Rossert, J. (2007). Scleraxis and NFATc regulate the expression of the pro-alpha1(I) collagen gene in tendon fibroblasts. *J. Biol. Chem.* **282**, 17665-17675. doi:10.1074/jbc.M610113200
- Logan, M., Martin, J. F., Nagy, A., Lobe, C., Olson, E. N. and Tabin, C. J. (2002). Expression of Cre recombinase in the developing mouse limb bud driven by a Prxl enhancer. *Genesis* **33**, 77-80. doi:10.1002/gene.10092
- Madisen, L., Zwingman, T. A., Sunkin, S. M., Oh, S. W., Zariwala, H. A., Gu, H., Ng, L. L., Palmiter, R. D., Hawrylycz, M. J., Jones, A. R. et al. (2010). A robust and high-throughput Cre reporting and characterization system for the whole mouse brain. *Nat. Neurosci.* **13**, 133-140. doi:10.1038/nn.2467
- Murchison, N. D., Price, B. A., Conner, D. A., Keene, D. R., Olson, E. N., Tabin, C. J. and Schweitzer, R. (2007). Regulation of tendon differentiation by scleraxis distinguishes force-transmitting tendons from muscle-anchoring tendons. *Development* **134**, 2697-2708. doi:10.1242/dev.001933
- Pryce, B. A., Brent, A. E., Murchison, N. D., Tabin, C. J. and Schweitzer, R. (2007). Generation of transgenic tendon reporters, ScxGFP and ScxAP, using regulatory elements of the scleraxis gene. *Dev. Dyn.* **236**, 1677-1682. doi:10.1002/dvdy.21179
- Schweitzer, R., Chung, J. H., Murtaugh, L. C., Brent, A. E., Rosen, V., Olson, E. N., Lassar, A. and Tabin, C. J. (2001). Analysis of the tendon cell fate using Scleraxis, a specific marker for tendons and ligaments. *Development* **128**, 3855-3866.
- Shinohara, H. (1999). The musculature of the mouse tail is characterized by metameric arrangements of bicipital muscles. *Okajimas Folia Anat. Jpn.* **76**, 157-169. doi:10.2535/ofaj1936.76.4_157
- Shwartz, Y., Viukov, S., Krief, S. and Zelzer, E. (2016). Joint development involves a continuous influx of Gdf5-positive cells. *Cell Rep.* **15**, 2577-2587. doi:10.1016/j.celrep.2016.05.055
- Soeda, T., Deng, J. M., de Crombrughe, B., Behringer, R. R., Nakamura, T. and Akiyama, H. (2010). Sox9-expressing precursors are the cellular origin of the cruciate ligament of the knee joint and the limb tendons. *Genesis* **48**, 635-644. doi:10.1002/dvg.20667
- Sugimoto, Y., Takimoto, A., Akiyama, H., Kist, R., Scherer, G., Nakamura, T., Hiraki, Y. and Shukunami, C. (2013). Scx+/Sox9+ progenitors contribute to the establishment of the junction between cartilage and tendon/ligament. *Development* **140**, 2280-2288. doi:10.1242/dev.096354
- Walthall, J. C. and Ashley-Ross, M. A. (2006). Postcranial myology of the California newt, *Taricha torosa*. *Anat. Rec. A Discov. Mol. Cell. Evol. Biol.* **288A**, 46-57. doi:10.1002/ar.a.20279
- Wang, L., Jiang, H. and Brigande, J. V. (2012). Gene transfer to the developing mouse inner ear by in vivo electroporation. *J. Vis. Exp.*, e3653. doi:10.3791/3653
- Watson, S. S., Riordan, T. J., Pryce, B. A. and Schweitzer, R. (2009). Tendons and muscles of the mouse forelimb during embryonic development. *Dev. Dyn.* **238**, 693-700. doi:10.1002/dvdy.21866
- Yoshimoto, Y., Takimoto, A., Watanabe, H., Hiraki, Y., Kondoh, G. and Shukunami, C. (2017). Scleraxis is required for maturation of tissue domains for proper integration of the musculoskeletal system. *Sci. Rep.* **7**, 45010. doi:10.1038/srep45010

Supplemental Files

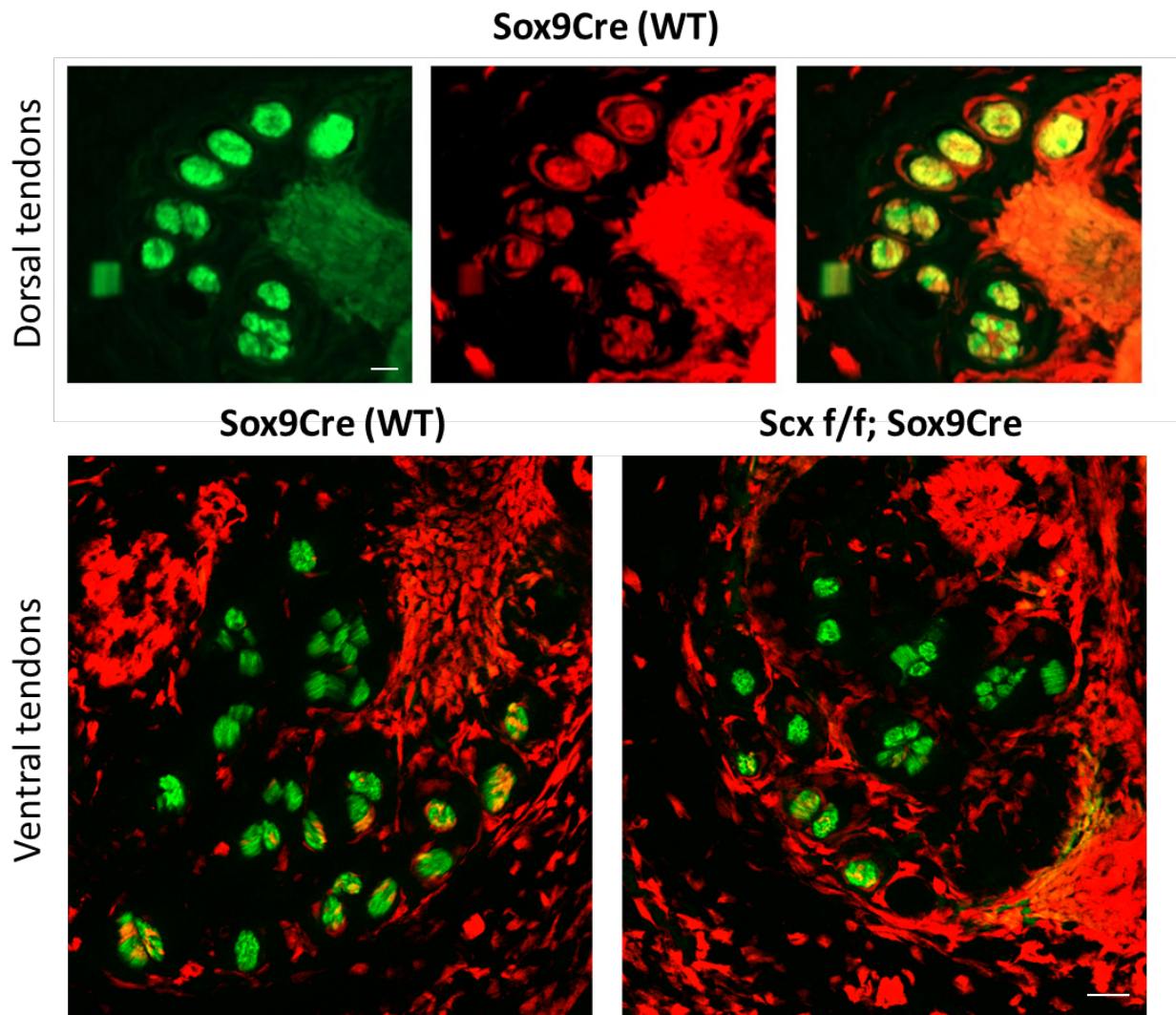
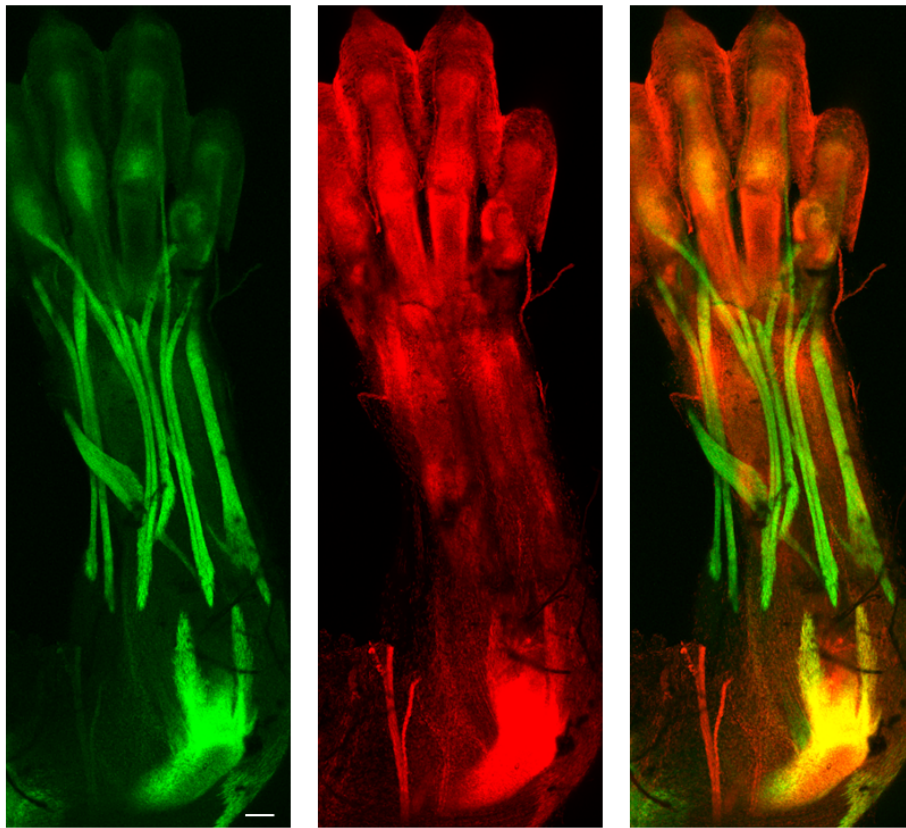


Figure S1: Lineage tracing reveals distinct contribution of *Sox9^{lin}* cells to dorsal and ventral tail tendons. Transverse sections through *Sox9^{Cre}; Rosa^T; ScxGFP* tails at E16.5 show that dorsal tail tendons are almost completely composed of *Sox9^{lin}* cells while ventral tail tendons are composed of a mixture of *Sox9^{lin}* and non-*Sox9^{lin}* cells. Transverse sections through *Scx^{Sox9Cre}; Rosa^T; ScxGFP* tails also show that mutant and wild type ventral tendons are similar in size. Scalebars: 25 μ m.

E15.5



E12.5

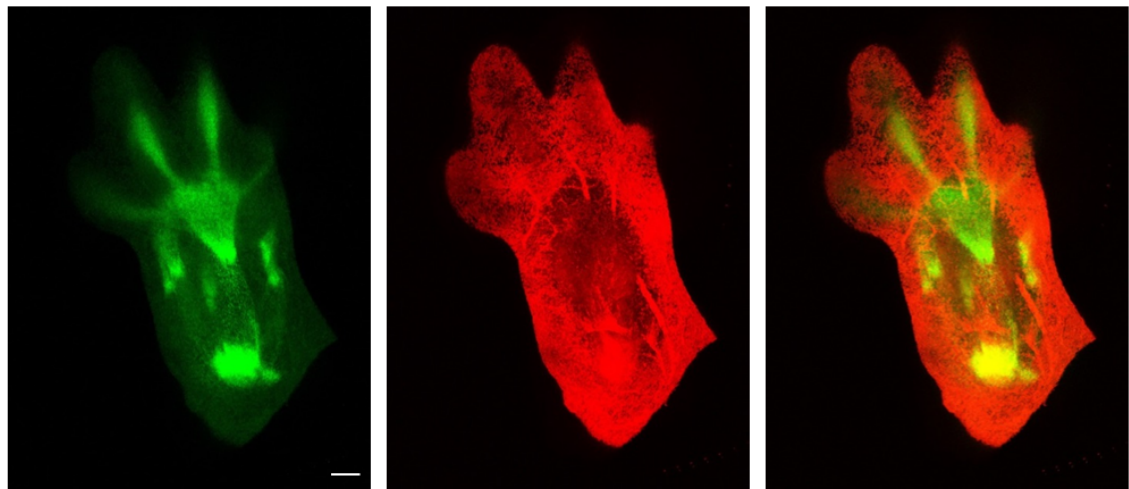


Figure S2: Unprocessed *Sox9^{Cre}*; *RosaT*; *ScxGFP* limbs at E15.5. Maximum projection images obtained from whole mount confocal microscopy shows overwhelming *RosaT* signal that is not restricted to tendon cells. Scalebars: 200 μ m.

Sox9Cre E12.5 (confocal zslice)

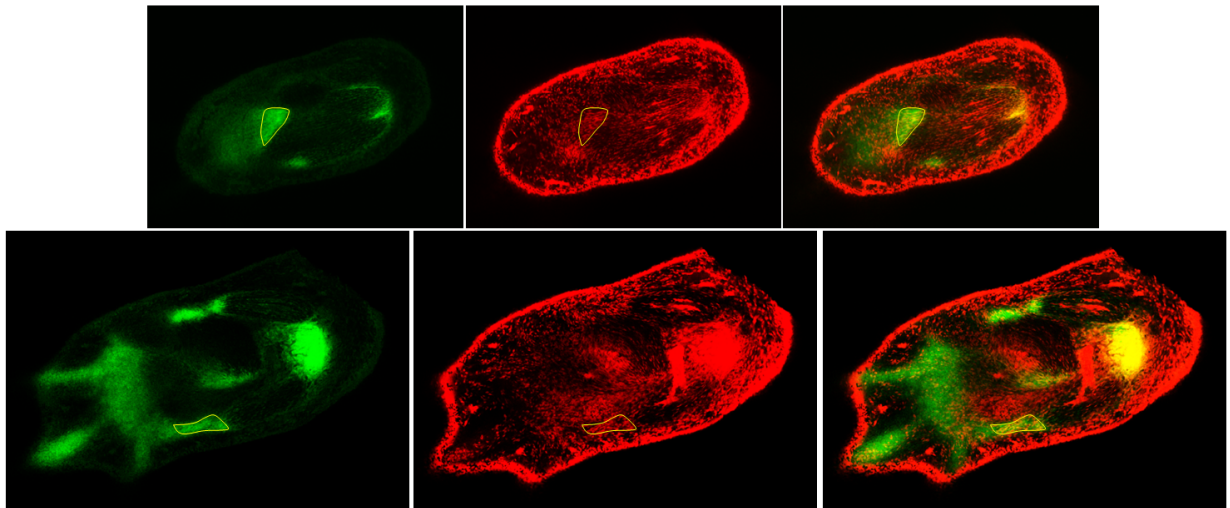


Figure S3: Unprocessed *Sox9^{Cre}*; *Rosa^T*; *ScxGFP* limbs at E12.5. Optical sections through the limb show concentration of *Sox9^{lin}* cells in short-range tendons near the wrist.